Photos: DOI: 10.2516/ogst/2013138, IFPEN, X.

Dossier

This paper is a part of the hereunder thematic dossier published in OGST Journal, Vol. 69, No. 3, pp. 379-499 and available online here

Cet article fait partie du dossier thématique ci-dessous publié dans la revue OGST, Vol. 69, n°3 pp. 379-499 et téléchargeable ici

DOSSIER Edited by/Sous la direction de : **J.-F. Argillier**

IFP Energies nouvelles International Conference / Les Rencontres Scientifiques d'IFP Energies nouvelles

Colloids 2012 — Colloids and Complex Fluids: Challenges and Opportunities

Colloids 2012 — Colloïdes et fluides complexes : défis et opportunités

Oil & Gas Science and Technology – Rev. IFP Energies nouvelles, Vol. 69 (2014), No. 3, pp. 379-499

Oil & Gas Science and Technology – Rev. IFP Energies nouvelles, Vol. 69 (2014), No. 3, pp. 415-434

DOI: 10.2516/ogst/2013147

Dossier

Colloids and Complex Fluids: Challenges and Opportunities
Colloïdes et fluides complexes : défis et opportunités

Freezing Within Emulsions: Theoretical Aspects and Engineering Applications

Danièle Clausse[1] and Christine Dalmazzone[2]*

[1] *Université de Technologie de Compiègne, Centre de Recherche, rue Personne de Roberval, BP 20529, 60205 Compiègne - France*
[2] *IFP Energies nouvelles, 1-4 avenue de Bois-Préau, 92852 Rueil-Malmaison - France*
e-mail: daniele.clausse@utc.fr - christine.dalmazzone@ifpen.fr

* Corresponding author

Résumé — **Congélation dans les émulsions : aspects théoriques et applications techniques** — Cet article se concentre principalement sur le comportement à la congélation des émulsions qui sont considérées soit comme des systèmes permettant d'obtenir des informations sur les matériaux en surfusion, soit comme des systèmes dispersés complexes impliqués dans les procédés industriels. En raison du fait qu'il existe une phase dispersée sous forme de fines gouttelettes dans les émulsions, des retards à la solidification sont observés et les gouttelettes de liquide persistent même en dessous du point de fusion du matériau. La corrélation entre la température de solidification des gouttelettes et leur taille peut être donc utilisée pour suivre l'évolution de la morphologie de l'émulsion en fonction du temps aussi bien sur terre que dans des conditions de microgravité (projet FASES soutenu par l'*ESA*). Une description de ces phénomènes observés principalement par microcalorimétrie sera donnée pour des corps purs dispersés ainsi que pour des solutions dispersées. Dans certains cas, les émulsions peuvent être recherchées pour leurs propriétés spécifiques, telles que la grande taille de l'interface huile/eau, conduisant à des transferts de masse améliorés; les émulsions peuvent être par conséquent utilisées comme des membranes liquides pour l'extraction, le stockage et la libération contrôlée de matières actives. Dans d'autres cas, la formation d'émulsions a un effet néfaste sur les procédés, comme dans l'industrie pétrolière où des émulsions eau-dans-pétrole très stables se forment facilement et compliquent l'opération de déshydratation du pétrole brut.

Abstract — ***Freezing Within Emulsions: Theoretical Aspects and Engineering Applications*** — *This article is mainly focused on the freezing behaviour of emulsions which will be considered either as systems permitting to get information about undercooled materials or as complex dispersed systems involved in industrial processes. Due to the fact that there exists a phase dispersed as tiny droplets in emulsions, solidification delays are observed and liquid droplets are still observed under the melting points of pure materials. The correlation between the solidification temperature of the droplets and their size may be therefore used to follow the evolution of the emulsion morphology* versus *time on ground as in microgravity conditions (FASES project supported by* ESA*). A description of these phenomena mainly observed through microcalorimetry experiments will be given for dispersed pure materials as for dispersed solutions. In some cases, emulsions may be sought after for their specific properties, such as their large oil/water interface, leading to enhanced mass transfers; emulsions may be consequently used as liquid membranes for extraction, storage and controlled release of active materials. In other cases, the formation of emulsions has a detrimental effect on the process. It is the case in the oil industry where very stable water-in-crude oil emulsions form easily and complicate the operation of crude oil dehydration.*

INTRODUCTION

Emulsions are well known systems as far as simple ones are concerned. They are obtained from the stirring of two bulk immiscible liquids, generally water and oil. Doing so, either water or oil is dispersed as droplets depending essentially on the relative amount of water and oil and the procedure used for mixing. Generally when stirring is stopped, the droplets either sediment or cream and coalescence of the droplets gives birth to two separated bulk phases as they were before mixing. To obtain an emulsion that shows a kinetic stability, namely a dispersion of droplets that will remain stable after stopping the stirring, it is necessary to add a component that will spread at the surface of the droplets avoiding their coalescence and therefore the breakdown of the emulsion. These components are referred as surfactant or more scientifically as amphiphilic products because they have the property of containing both a hydrophilic and a lipophilic moiety. In order to satisfy this property, these molecules will be preferably found at the Water/Oil (W/O) interface of the droplets. Theoretically it can be shown that these components decrease the surface energy of the droplet and therefore the total energy of the system leading to a kinetic stability. More details about these aspects may be found on general treatises about emulsions, as the basic one written by Becher [1] and as some more recent ones [2-6].

Less known are the so-called double or multiple emulsions. They are obtained by dispersing an already formed emulsion in a continuous phase corresponding to the dispersed phase of the emulsion. Thus a W/O emulsion dispersed in water is referred as a Water-in-Oil-in-Water emulsion (W/O/W), while an O/W emulsion dispersed in oil corresponds to a O/W/O emulsion. Double or multiple emulsions are among the most used for either entrapping active products or performing liquid/liquid separations. Depending on the end use, the formulation may include two surfactants to get a kinetically stable emulsion for entrapping active products or only one for improving separation processes, the breakdown of the multiple emulsion being generally required at the end of the process. A general description of uses of these emulsions for entrapping or release of products can be found in [7-42] as they have been considered as emulsified liquid membranes showing a huge separation exchange membrane that can be estimated by the areas of the surface droplets. For instance, starting from a surface area of 1 cm^2 which separates two equal volumes of oil and water bulk phases, the total volume being one cm^3, the emulsification into monodisperse droplets of 1 μm radius will lead to an increase of the total interfacial area up to around 10^4 cm^2.

Close to simple emulsions but different inasmuch as they contain two populations of droplets of different composition, we find what has been referred as mixed emulsions. They have been also considered as systems showing liquid membranes, but easier for controlling stability, and as a possible way to control the droplets size [43-57]. They are obtained by gentle mixing, in order to avoid coalescence between droplets, of two simple emulsions containing droplets of different composition. The evolution of this kind of emulsions due to a possible mass transfer between droplets of different composition will be described in this article.

Solidification and melting occurring in the emulsions described above will be reported first. Some results obtained by Differential Scanning Calorimetry (DSC) that permits to detect the thermal energies either released or absorbed during either freezing or melting will be given. From this analysis it will be shown that monitoring the changes of the solidification temperatures *versus* time is a way to get information about the evolution of the emulsions in terms of stability and mass transfers. Some examples will be given to illustrate these phenomena, one concerning the study of the evolution of emulsions in microgravity conditions (FASES project supported by ESA – European Space Agency) [58, 59] and the others dealing with other applications including the petroleum industry.

1 SOLIDIFICATION AND MELTING WITHIN EMULSIONS

The ways solidification and melting occur within emulsions have been described thoroughly in previous articles [6, 60-65]. Only the main points needed to understand the phenomena linked with them will be recalled in this article. After giving some details on the technique used to show these thermal events, namely Differential Scanning Calorimetry (DSC), some illustrative experimental results will be given. As the structure of the kind of emulsion under study leads to different results, simple, multiple and mixed emulsions will be treated separately.

1.1 Theoretical Aspects

Within emulsions, two types of phases are encountered: a continuous one referred also as the bulk phase and a dispersed one concerning all the droplets. Therefore, solidification and melting of these two types of phases can occur assuming of course that during the temperature scanning, these phases may undergo liquid/solid changes of state. Knowing the materials used for making the emulsions, it is possible to find the thermodynamic data about melting from the literature. More complicated

and even often impossible to find in the literature are the data about solidification. This is due to nucleation phenomena that induce delays which depend not only on the volume of the studied sample but also on the used scanning rate. And even if these parameters are well identified, no universal correlation is available and they have to be set up for the system under study. In this article, the properties of solidification of a single sample considered as the continuous phase of an emulsion will be described first. Afterwards the solidification of several samples simulating the droplets within the emulsion will be described.

1.1.1 Solidification of a Single Sample

The main point to have in mind is that it is not possible to consider that the whole phase submitted to a regular cooling will solidify instantaneously and totally when the melting point is reached, namely 0°C for water under atmospheric pressure. At least a previous solid embryo which has the structure of the solid to be formed has to be created, and furthermore it has to be larger than a critical size to grow, otherwise it will disappear. The embryo of critical size is referred as a germ. Its formation is the result of local fluctuations of density and therefore it has necessarily a size relevant to what is called colloidal particles for which capillary aspects have to be taken into account. The main point is that, due to the great curvature of the germ surface, the pressure inside the germ P_s is larger than the one of the surrounding liquid P_l according to the Laplace law:

$$P_s - P_l = \frac{2\gamma}{R} \tag{1}$$

γ being the interfacial energy between the germ and the surrounding liquid and R being the radius of the germ.

Therefore, what could be called a metastable equilibrium between the solid germ and the surrounding liquid can only be achieved when the temperature is lower than the one corresponding to the equilibrium between a macroscopic solid of infinite radius and the liquid. Nucleation in a sample has been thoroughly described in basic books dealing with the nucleation of a liquid droplet [66-71] in a supersaturated vapor. Fewer studies are devoted to the nucleation of a solid in a liquid due to the problem for defining a solid germ and its properties, the pioneers in the field being Turnbull [72], Dufour and Defay [66] and Pruppacher and Klett [68]. Nevertheless these theories have been successfully applied to nucleation in condense systems and they give reliable information about the thermodynamic properties of the equilibrium between the solid germ and the undercooled liquid. They include also the concept of the nucleation rate J defined as the number of germs formed by time unit and volume unit. This parameter traduces the fact that as the germs are the result of density fluctuations in the undercooled liquid, their formation must be described in terms of probability. J can be expressed simply in terms of an activated phenomenon according to an exponential law when in fact the phenomenon itself is much more complicated. A positive energy E has to be overpassed, its expression showing its dependence with the germ radius to be formed being given by:

$$E = \frac{4}{3}\pi\gamma R^2 \tag{2}$$

The expression of J *versus* E is written as:

$$J = A \exp\left(-\frac{E}{kT}\right) \tag{3}$$

A being a parameter depending essentially on viscosity, k the Boltzmann constant and T the temperature in Kelvin. This formula traduces the expected fact that the smallest R is, the highest J is. The thermodynamic study of the system shows that R is the biggest when the difference between the melting temperature T_m and the temperature T is the smallest in agreement with the fact that for $T = T_m$ the radius can be considered as infinite. It follows that E is infinite and $J = 0$. Solidification at T_m appears as difficult to obtain spontaneously and when solidification is required in industrial applications, nucleation is provoked and therefore under control by adding specific materials that will induce the nucleation. Of course the best material to do so should be a particle of the material itself. That is the process used for solidification of materials such as NaCl in an aqueous solution. But very often in the conditions in which nucleation has to occur, solid particles are not available. It is the case for the formation of ice from undercooled water at a temperature less than 0°C and solid particles showing the best isomorphism with the solid to be formed have to be found. A well known nucleation initiator for ice is silver iodide. Many studies have been undertaken with this material in the field of meteorology. For the time being the results are not completely satisfactory as far as it has been shown that the probabilistic character of nucleation remains. The required energy is of course less but not enough to suppress this aspect [73].

The ways to freeze and melt a solution are much more complicated in comparison to what has been described for a pure compound insomuch as two compounds are present and may crystallize or melt at

different temperatures. Furthermore the behavior can be different depending on the relative solubility of one of the compound in the other. In this article, we only present the already complicated problem where the solid phases are pure crystals and where there is an eutectic equilibrium. That is generally the case for water + salt binary systems.

1.1.2 Several Samples: Droplets of an Emulsion

The simplest model is to consider that the whole droplets have the same radius r, not to be confused with the germ radius R needed for initiating the solidification of the droplet.

Pure Compound (during a regular cooling)
In this section, we present the case of the crystallization of droplets which are supposed to be sufficiently distant from each other to ignore thermal effects. It would, for example, be the case of droplets in clouds or in very slightly concentrated emulsions.

Let us suppose that all droplets, in number N_0, have the same volume V_0. They are dispersed within an emulsion which is regularly cooled at a constant cooling rate β (<0 for a cooling). During this cooling, germs are formed and droplets freeze assuming that freezing takes place as soon as a germ is formed. It is noteworthy that Equation (3) gives the number of germs formed per second in a volume unit, but it does not give any information about where in the volume these germs are formed. Therefore the appearance of a germ and by the way the freezing of a droplet is a 'random phenomenon' leading to a scattering of the freezing temperatures even for droplets having the same volume V_0. Nevertheless the dispersion of the freezing temperatures does not prevent the recognition of a very characteristic mean value which has been called the mean freezing temperature according to Dufour and Defay [66]. Another temperature has been introduced more for commodity reasons than for theoretical ones linked to the experimental procedure used to study a great number of droplets as it is the case in an emulsion. This temperature has been referred in the literature as the most probable freezing temperature T^* [60, 61, 74-76].

Let be dN the number of droplets that freeze during cooling either between times t and $t + dt$ or between temperatures T and $T + dT$. Namely,

$$dN = N(t + dt) - N(t) = J(t)V_0[N_0 - N(t)]dt \quad (4)$$

or

$$dN = N(T + dT) - N(T) = J(T)V_0[N_0 - N(T)]\frac{dT}{|\beta|} \quad (5)$$

In Equation (5), N_0 and β are constants, and $J(T)$ and $N_0 - N(T)$ vary from 0 to ∞ and from N_0 to 0, respectively, when T decreases during the cooling down to a temperature at which all the droplets are frozen. Therefore, a maximum in $\frac{dN}{dT}$ is expected, which corresponds to T^*.

Pure Compound (at a fixed temperature $T \leq T_m$)
In the preceding section, the way the droplets freeze during a steady cooling has been described. Another way to obtain their freezing is to maintain the emulsion at a fixed temperature T below the melting temperature, namely 273.15 K for a W/O emulsion.

The great advantage to do so is that the nucleation rate J is a constant *versus* time and the integration of relation (4) is straightforward as far as it is assumed that at time 0, all the droplets are liquid when T is not too close to T^*:

$$\ln\left(1 - \frac{N}{N_0}\right) = -JVt \quad (6)$$

When the model is validated, it is possible to get J by performing experiments that will give the percentage of frozen droplets N/N_0 *versus* time. By plotting $\ln(1 - N/N_0)$ *versus* time the slope of the straight line will give JV and therefore J for a known volume V. This method has been used for getting the value of the interfacial energy γ of the surface between the germ and the undercooled liquid, value which cannot be determined directly [64, 72].

The model described before can be improved by introducing in the equations the polydispersity of the droplets described by an analytical function. An example of such a determination can be found [60, 74] by using the following analytical function:

$$g(D) = \frac{1}{dD}\frac{dN}{N} = 2\frac{D^2}{D_p^3}\exp\left[-\frac{2}{3}\left(\frac{D}{D_p}\right)^3\right] \quad (7)$$

In this relation, g gives the proportion of droplets the diameter D of which is included between D and $D + dD$, D_p being the mean diameter and N the total number of droplets under study. It has been found that this relationship is suitable for a water-in-oil emulsion whose polydispersity has been determined by the freeze fracture technique [74].

The proportion of crystallized volume $Z(t)$ given by:

$$Z(t) = \sum_{dN}\frac{VdN(V,t)}{V_{total}} \quad (8)$$

can be expressed as:

$$Z(t) = 1 - \frac{1}{\left(1 + 3\frac{V_p}{2}J(T)t\right)^2} \quad (9)$$

V_p being the mean volume deduced from the polydispersity analysis (*Eq.* 7).

Binary Compound

Let us now examine the case of a solution of two compounds $A + B$ which is dispersed as droplets within an emulsion. The way the droplets solidify during a steady cooling can be deduced from what has been described for a single sample of volume V and for droplets of a pure material of same volume V dispersed within an emulsion. In that case a mean temperature of solidification of either A or B can be introduced and the phases diagram can be completed as it appears in Figure 1 [65].

The composition is given by the molar fraction x_b of component B. The equilibrium curves are given by the solid line while the mean solidification temperatures are given by the dotted lines. Note that these mean solidification temperatures may be easily determined by a single DSC test on a monodisperse W/O emulsion sample, as the high number of droplets dispersed in the emulsion allows a statistical treatment of the solidification temperatures of all the droplets (see *Sect. 1.2*). For $x_b = 0$, it is the mean solidification temperature of the pure component A which is given, while for $x_b = 1$, it is the one of pure component B. For example, for an aqueous solution of NaCl dispersed as micro size droplets, the point on the axis $x_b = 0$ will give –40°C for pure water. For a dispersed solution the composition of which is given by the abscissa of point A^e, only the solid phase A appears first and the mean crystallization temperature is given by the ordinate of point A. A certain amount of solid phase will form until the composition of the remaining solution reaches the one given by the abscissa of point A' belonging to the extension of the equilibrium curve solid A + solution, *i.e.* Γ_e. The total solidification will be obtained at a lower temperature at a point indicated as $(B+A)$ in Figure 1. A similar behavior is obtained when solid B appears first. The great advantage of studying the behavior of a population of droplets, which is the case when emulsions are concerned, is that the dotted lines Γ and Σ can be obtained experimentally and their knowledge permits to predict how the solidification of droplets will occur *versus* their composition. These curves are not equilibrium ones and therefore they are dependent on the cooling rate and the droplets sizes. Nevertheless, as it has previously been underlined for a pure disperse material, they can show an evolution of the emulsion due to the changing of the droplets sizes. Furthermore a change in the composition can be followed through the change of the mean solidification temperatures of the droplets. This property has been used to follow mass transfers in emulsions between phases of different compositions as it will be shown in the section devoted to applications.

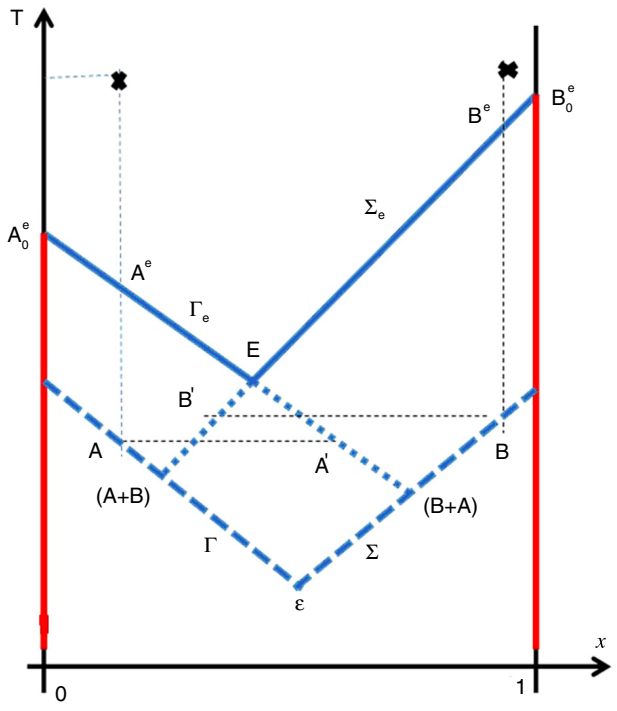

Figure 1

Phase diagram for a supercooled binary system $A + B$. Solid line: solid-liquid equilibrium curves, solid $x_b = 0$, liquidus Γ_e for $x < x(E)$; solid $x_b = 1$, liquidus Σ_e for $x > x(E)$, with E: eutectic point. Dotted line: most probable solidification temperatures for dispersed solutions within emulsions: A solidification: Γ; B solidification: Σ; complete solidification points $(A + B)$ and $(B + A)$.

1.1.3 Solidification Within Multiple Emulsions

As it has been described in the Introduction, two kinds of multiple emulsions may be encountered, *i.e.* W/O/W or O/W/O.

Let us first consider W/O/W emulsions for which water droplets are dispersed within oil globules themselves being dispersed within an aqueous phase. Each oil globule can be considered as a W/O emulsion and the rules for solidification are the same as the ones described in the preceding section for a W/O emulsion. For the bulk aqueous phase in which the oil globules are dispersed, the rules of crystallization/melting are

the same as the ones described for a unique sample, assuming that the presence of the oil globules has no influence on the nucleation. Nevertheless, as the probability of nucleation is higher for the bulk aqueous phase than for the smaller disperse droplets, it is expected that the nucleation will be observed first in the bulk and later on in the droplets. This situation may have an effect on the further nucleation of the droplets due to a mass transfer from the already frozen bulk phase to the still liquid droplets. An example of this phenomenon will be given in the section devoted to mass transfer within emulsions.

For O/W/O emulsions, the droplets in the aqueous globules are made of oil, the globules being themselves dispersed within an oil medium. Even if they contain oil droplets, the water globules are expected to crystallize at a mean temperature which is dependent on their volume as it has been stressed in the section devoted to the descriptions of the rules of droplets crystallization. Should the oil phases (droplets and bulk) undergo solidification, the rules will be the same as the ones presented for W/O/W emulsions.

1.1.4 Solidification Within Mixed Emulsion

These emulsions have been described in the introduction. In so far as they contain two populations of droplets of different compositions, the crystallization and the melting will occur at temperatures which depend on the composition of the droplets as it has been described in the section devoted to crystallization and melting of droplets from binary solutions. Therefore it is expected that the droplets crystallize around two different mean temperatures based on their composition. This result has been used to follow the possible mass transfer at ambient temperature due to the difference of composition, the emulsions being considered as systems showing liquid membranes. Examples will be given in the section on mass transfer within emulsions.

1.2 Experimental Results

This section describes some results essentially obtained by Differential Scanning Calorimetry (DSC). The principle of the technique is based on the monitoring of the energy which is either released or absorbed during freezing or melting of an emulsion sample that has been poured in a crucible and inserted in the head of a calorimeter. This technique has been described thoroughly elsewhere [59, 62, 63, 65] for such determinations. Referring to different kinds of emulsions as described before, signals showing the progressive freezing of either the dispersed droplets or bulk phases present in the emulsions are expected. Typical freezing curves observed for pure compounds are given in Figures 2 and 3.

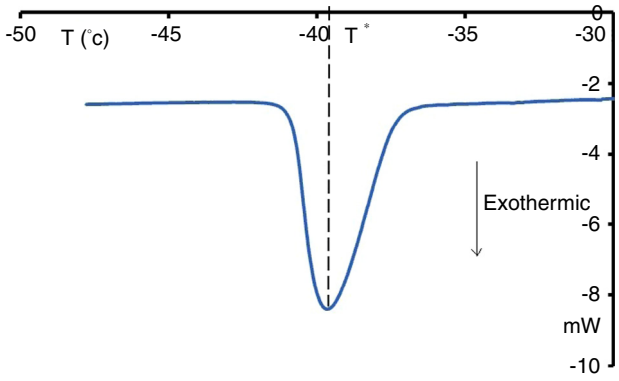

Figure 2

Freezing curve of a water-in-oil (W/O) emulsion (heat flow *versus* temperature, exothermic signal downwards).

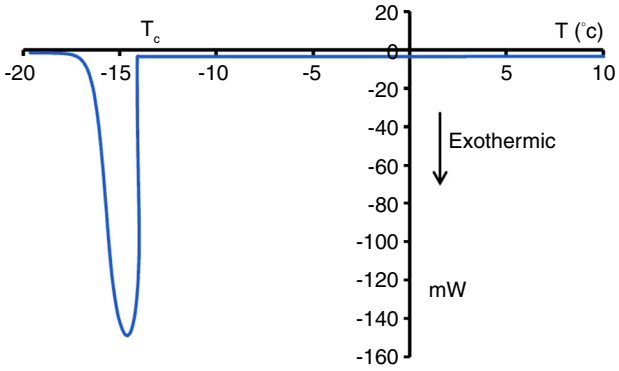

Figure 3

Freezing curve of a water bulk sample of a few mm^3 (heat flow *versus* temperature, exothermic signal downwards).

Microscopic observation made on emulsions have shown that Figure 2 is characteristic of water droplets whose radius is around 1 μm. The number of droplets dispersed in the sample of emulsion of a few milligrams is very high and sufficient to allow a statistic treatment of the various solidification temperatures of the whole droplets. The energy released during the droplets freezing is evidenced on the obtained thermogram as an exothermic peak with a quite perfect bell shape as the emulsion is monodisperse. The apex temperature of the peak corresponds to the most probable temperature of solidification T^* and may be correlated to the mean droplet size.

Figure 3 has been retained as characteristic of a completely destabilized W/O emulsion showing a bulk water phase. Only one germ may initiate the solidification and once nucleation occurs, the complete process of crystallization is very fast. Therefore a significant amount of energy is released in a very short time, and that is the reason why the first part of the exothermic freezing peak is so sharp. Note that the freezing temperature T_c is expected to vary from one sample to another, because nucleation is a stochastic phenomenon.

Should the emulsion evolve with time, intermediate signals between these two given by Figures 2 and 3 will be observed. That is the basis of the technique proposed for monitoring the evolution of W/O emulsions in microgravity conditions. This study named FASES project supported by *ESA* is described elsewhere [59]. For the time being only results obtained on ground are available, experiments in the FSL (Fluid Science Laboratory) having not yet been performed. The aim of the study is to see the influence of gravity through sedimentation and convection on the evolution of emulsions by observing the changes of the droplets freezing temperatures *versus* time. An example of experiments on ground are given in Figure 4 for fresh emulsions ($t = 0$ day), and after storage at room temperature during several days (1, 2 and 15 days).

These curves clearly show that there is a significant change of the emulsion with time, the freezing signals being shifted to higher temperatures between 0 and 15 days. This is in agreement with dispersed water showing increasingly big droplets, due to coalescence phenomena. For $t = 15$ days, it is noticeable that even a part of the initially completely dispersed water ($t = 0$ day) partially appears as a bulk phase, as evidenced by the signal which starts at –20°C and shows a steep slope as in Figure 3. Note that in the case of the bulk phase the starting point of the signal can change even for a same sample due to the random character of nucleation phenomena, as it has been described in the section devoted to the solidification of single samples.

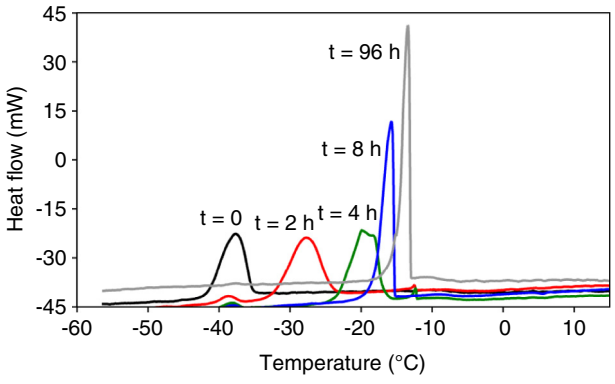

Figure 4

Evolution with time of the freezing curves for W/O emulsions (heat flow *versus* temperature, exothermic signal upwards).

The freezing and melting curves expected when a solution is dispersed (instead of a pure compound) are schematically given in Figure 5.

One or two signals can be obtained depending on the composition of the solution under study and the temperature reached during cooling. For a population of samples as it is the case for droplets dispersed within an emulsion, a distribution of the solidification temperatures has to be taken into account as for droplets made of a pure material. Therefore, the freezing curve obtained by DSC will show one or two signals due to the solidification of either *A* or *B* followed or not by a signal at a lower temperature due to the complete solidification of the remaining solution existing after the previous solidification in agreement with the theoretical description made in section on binary compounds. The mean freezing temperatures obtained by taking the temperatures of the apex of the freezing signals [65] allow to draw curves representing the behavior described in section on binary compounds. The results obtained depend on the composition and the temperatures reached during cooling are described schematically in Figure 5 for 6 compositions indicated by dotted lines. The composition is given by the molar fraction of component *B*. Curves $A_0^e E$ and $B_0^e E$ are the equilibrium curves that give the *A* solidification points and the *B* solidification points respectively. These curves join together at the eutectic point *E*. When a solution is dispersed within an emulsion the solidification of the droplets shows different results depending on the composition. A composition, different from the eutectic point *E*, separates the sequence of the events. This point indicated as ε on the graph is found at the intersection of two lines that give the mean solidification temperatures of *A* for $x < x_\varepsilon$ and the mean solidification temperatures of *B* for $x > x_\varepsilon$. The circles mimic the contents of the droplets regarding the solid materials present. They are drawn in front of the respective signals shown by DSC. For example for droplets whose composition is given by dotted line 2, the cooling curve exhibits two signals, one showing the partial solidification of *A* and at a lower temperature the total solidification of the droplet, namely the solidification of *B* and the solidification of the remaining *A* which is still liquid. As it can be seen on the diagram, the signals shift with the composition. The temperature of the apex of the

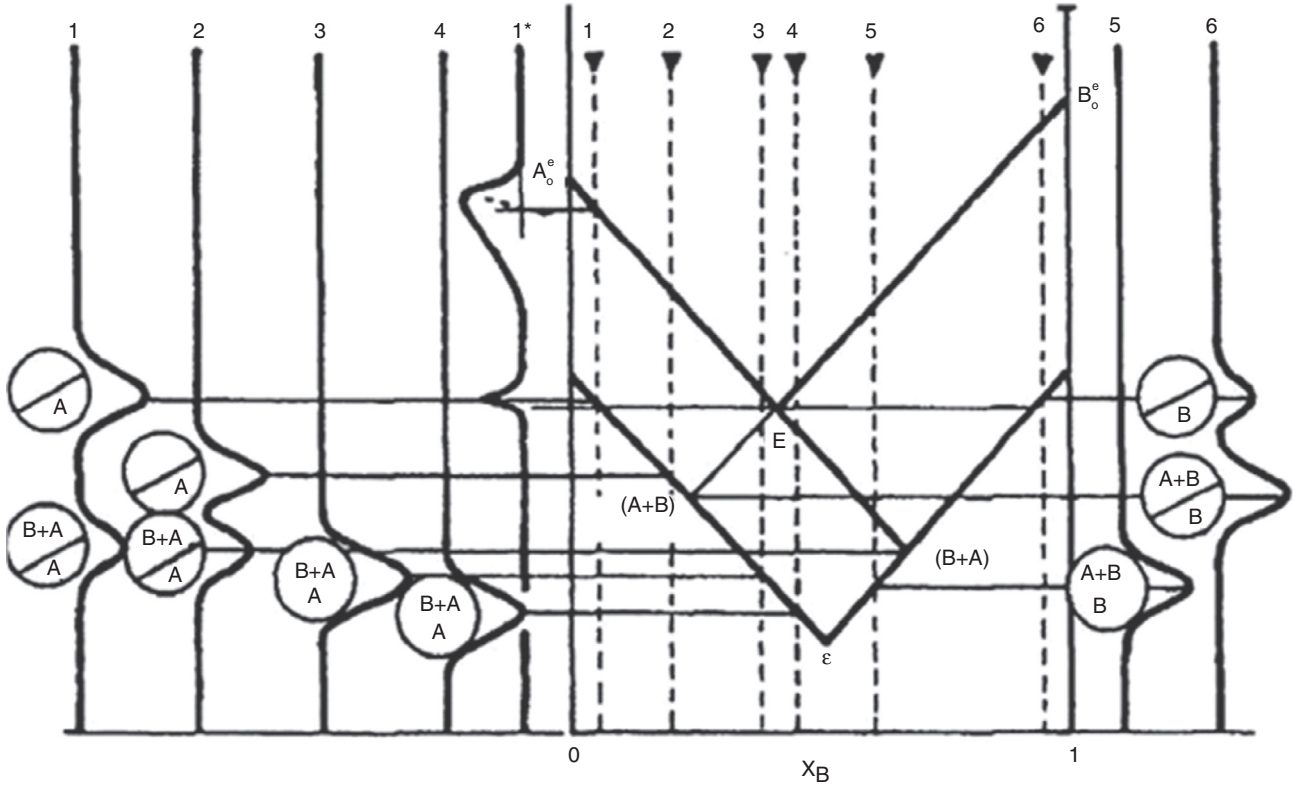

Figure 5

Schematic binary system $A + B$, with cooling DSC curves and droplets solid contents at 6 compositions of dispersed solution within emulsions and with melting DSC curve at composition 1* (for practical reasons of clarity, the thermograms are vertical).

first signal observed gives the mean solidification temperature as it was yet described for dispersed pure material. The heating curve represented in Figure 5 by the line 1* for the composition represented by the dotted line 1, shows the eutectic melting followed by the progressive melting of component *A* until its complete dissolution when the equilibrium line is reached. This diagram is a schematic one for the case considered, *i.e.* solutions that can be mixed in all proportions and that show an eutectic point. Generally, especially for (water + salt) systems, the diagram is limited because very concentrated solutions of *B* are impossible to reach.

An example of such behavior has been obtained for the binary (NH_4Cl + H_2O) solutions dispersed within an emulsion (*Fig. 6*) [6].

The results dealing with a solution of molar fraction x higher than the one corresponding to the saturation at 20°C have been obtained by using a process involving mass transfer of water in the emulsion, as solutions do not bear high temperatures due to decomposition. To do so, an emulsion containing a dispersed solution of molar fraction $x_0 = 0.100$, *i.e.* undersaturated at 20°C, is placed in a rather dry atmosphere in order to provoke the evaporation of the droplets by regular agitation. The emulsion under study is regularly weighted in order to know the amount of evaporated water and to deduce the actual molar fraction of the droplets. It was surprising to see at this time that the evaporation which is a result of a mass transfer of water in the oil medium was occurring quite homogeneously in the emulsion. This point was checked by performing a DSC test on a sample taken from the mother emulsion submitted to evaporation. The signal obtained was the one obtained by studying an emulsion made with a solution directly dispersed in the oil medium and having the molar fraction of the mother emulsion under study.

The temperatures of the apex of the various signals obtained during cooling are indicated as crosses in Figure 6. Depending on the composition, one, two or even three signals can be observed in agreement with the theoretical presentation of the expected results indicated in Figure 6. The third one specific to the binary

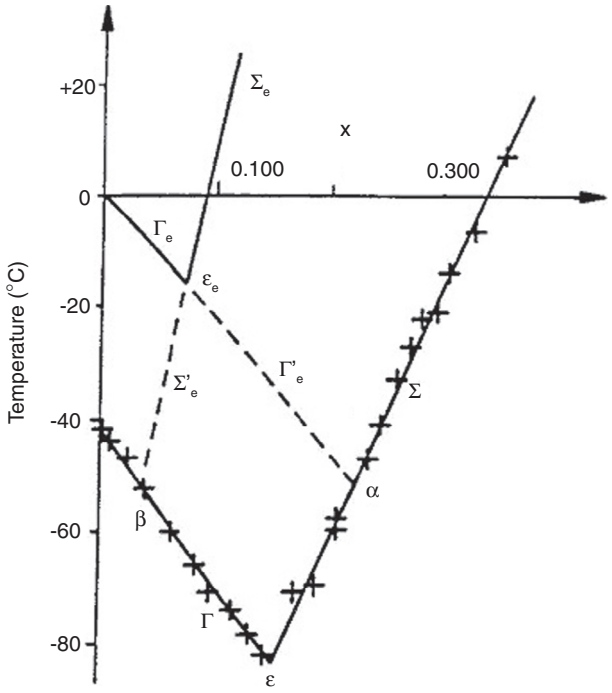

Figure 6

Freezing curves for the binary $NH_4Cl + H_2O$ dispersed within a W/O emulsion.

under study is the one corresponding to thermal transition at –31°C. Curve Γ is not an equilibrium curve but it gives the points at which ice first appears in the droplets while curve Σ gives the points at which salt appears first in the droplets. They join at point ε that reminds the eutectic point ε_e but which is not an equilibrium point and furthermore which does not show the same composition. The degrees of undercooling given by curve Γ vary between 40°C (pure water) and 49°C for $x_0 = 0.15$ and the degrees of supersaturation given by curve Σ vary between 145°C for $x_0 = 0.16$ and 211°C for $x_0 = 0.35$.

2 APPLICATIONS

This section presents applications in the field of mass transfer and crude oil production.

2.1 Mass Transfer

An application of the results obtained by studying the freezing and melting occurring within emulsions concerns the mass transfer within emulsions. More details about these transfers can be found in references [26-28, 43-45, 48-51, 55].

2.1.1 Mass Transfers Within Mixed Emulsions

In the case of W/O mixed emulsions containing pure water droplets and aqueous urea solution droplets stabilized by lanolin surfactant, the DSC cooling curves (*Fig. 7*) indicate two solidification peaks corresponding to the freezing signal I of pure water droplet at $T_c = -39$°C (*Fig. 7a*) and the freezing signal II of aqueous urea solution droplets with a concentration of 30 wt% at $T_c = -60$°C (*Fig. 7b*). DSC cooling curves point out a noticeable decrease of the signal I area with time characteristic of pure water droplets freezing (*Fig. 7c, d*). In addition, DSC cooling curves show a shift with time towards higher temperature for the signal II corresponding to the solidification of (water + urea)

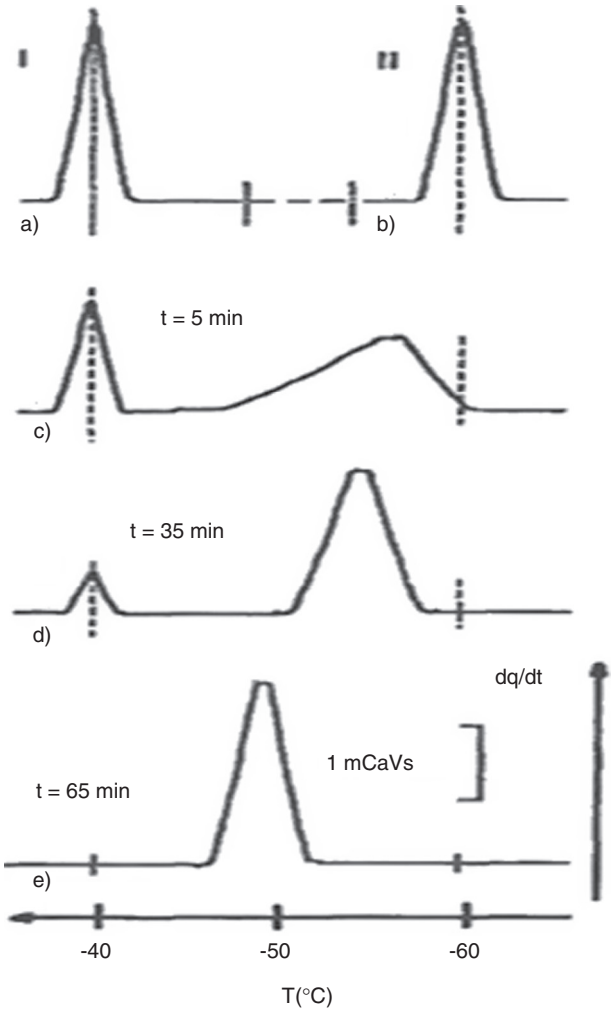

Figure 7

DSC cooling curves of W/O mixed emulsion with pure water droplets a) and water + urea droplets b) dispersed in oil media at successive time intervals c) $t = 5$ min; d) $t = 35$ min; e) $t = 65$ min, exothermic signal upwards (from [48]).

droplets. Therefore these results evidence that there is no urea transfer and that water has been transported from the pure water droplets towards the (water + urea) droplets, causing their dilution, according to the calibration curve of this system reported in Figure 8. Finally, only one signal at around T = –48°C is observed 65 min after the mixing and no more evolution has been observed after that time (*Fig. 7e*). This unique signal suggests that there are no more pure water droplets whereas the (water + urea) droplets are still present, their dilution having reached a maximum. From the knowledge of the dependence of the (water + urea) droplets freezing temperature *versus* the urea composition (*Fig. 8*), it was deduced that the unique signal observed at T_c = –48°C is characteristic of the freezing of 15 wt% urea solution droplets. This final composition is in agreement with the initial W/O mixed emulsion obtained by mixing equal masses of each W/O simple emulsion containing 30% of pure water droplets and 30% of aqueous urea solution droplets. The evolution of pure water moles numbers in mixed emulsion was deduced from the surface area of the solidification signal I of pure water (*Fig. 9*). The water transfer can be modeled by an homogeneous solution-diffusion model [48].

In the case of W/O mixed emulsions containing pure water droplets and aqueous NaCl solution droplets stabilized by lanolin surfactant, the DSC cooling curves (*Fig. 10*) indicate a solidification signal I at T^* = –39.5°C corresponding to freezing of pure water droplet (*Fig. 10a*) and a solidification signal II relative to the freezing of aqueous NaCl solution droplets with a concentration of 20 wt% at T_c = –67°C (*Fig. 10g*). With time, DSC cooling curves show a decrease of the area of the solidification signal I of pure water droplets whereas the freezing signal II appears to broaden first and then to be more and more narrow (*Fig. 10a-e*). These results evidence the decrease of the amount of pure water droplets in the mixed emulsion by a dilution of the water + NaCl droplets by the water coming from the pure water droplets. After 82 min, the DSC cooling curves do not change any more and the signal I has practically disappeared while a well defined signal II observed at around T_c = –51°C is noticeable (*Fig. 10e*). This unique signal evidences that the complete water mass transfer is achieved: no more pure water droplets are still present and the (water + NaCl) droplets are diluted as much as possible. From the knowledge of the phase diagram of the water + NaCl emulsified system, and the melting temperature of the final droplets population, it was deduced that the unique signal observed at –51°C is characteristic of the freezing of 10 wt% aqueous NaCl solution droplets. This final composition is in agreement with the formulation of the W/O mixed emulsion. The evolution of the percentage of pure water moles numbers in mixed emulsion was deduced from the surface area of the solidification signal I of pure water (*Fig. 11*).

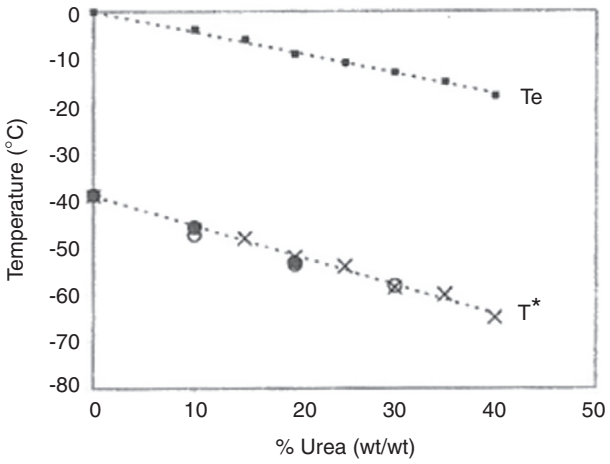

Figure 8

Freezing temperature of urea solution *versus* urea concentration. *Te*: equilibrium freezing temperature of the urea solution in bulk; *T**: temperature of crystallization of the micro-sized droplets of urea solution dispersed in oil media (from [48]).

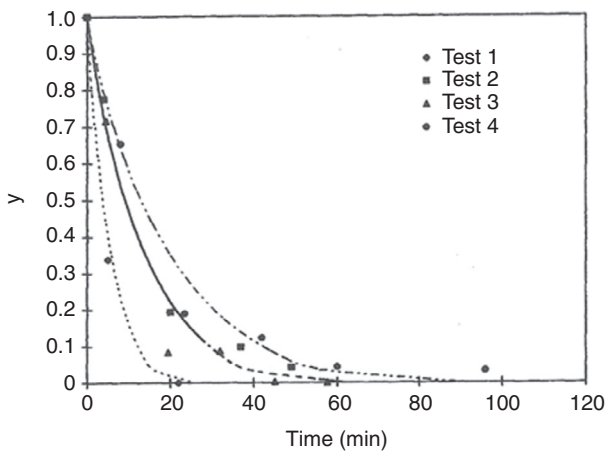

Figure 9

Percentage y of pure water moles numbers transferred in W/O mixed emulsion with pure water droplets and water + urea droplets dispersed in oil media *versus* time (from [48]).

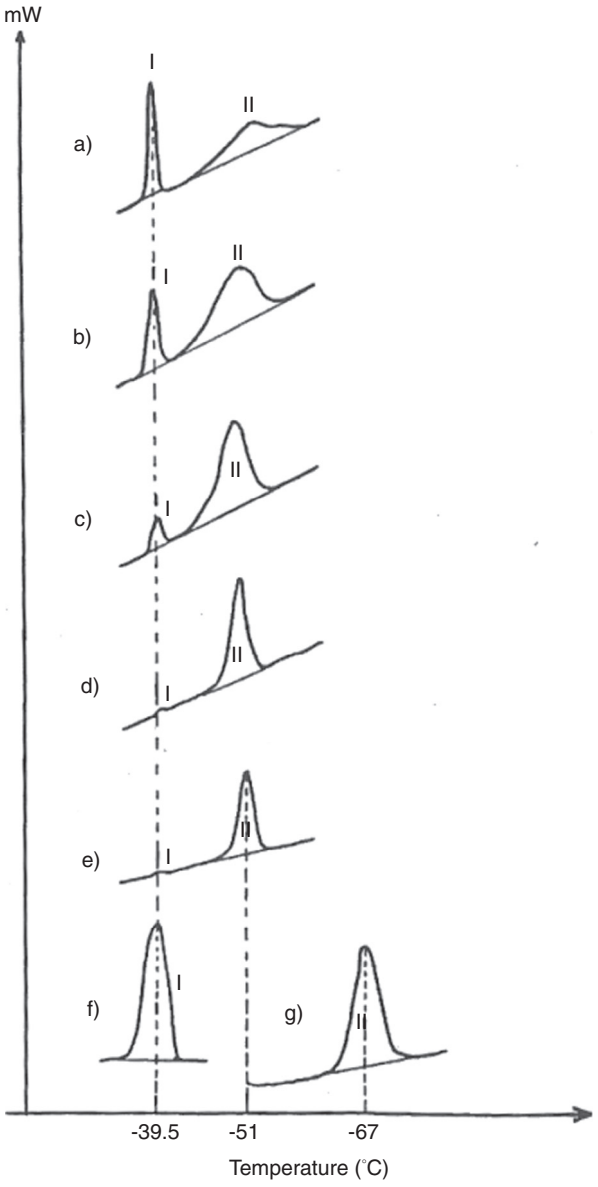

Figure 10

DSC cooling curves of W/O mixed emulsion with pure water droplets and water + NaCl droplets dispersed in oil media at successive time intervals a) t = 2 min; b) t = 25 min; c) t = 43 min; d) t = 62 min; e) t = 82 min after the mixing of f) emulsion 1 (pure water and g) emulsion 2 (water + NaCl) (from [49]).

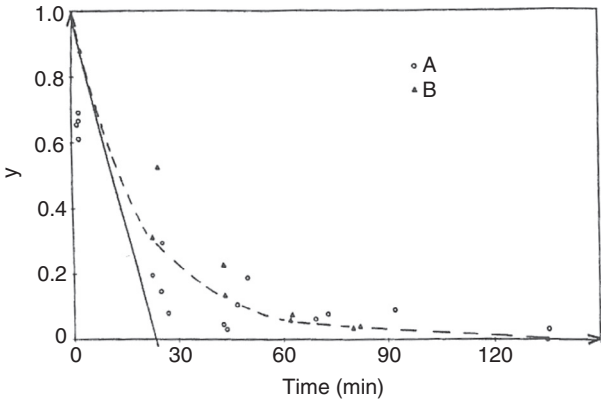

Figure 11

Percentage y of pure water moles numbers transferred in W/O mixed emulsion with pure water droplets and water + NaCl droplets dispersed in oil media (oil A or oil B), *versus* time (from [49]).

In the case of W/O mixed emulsions containing pure water droplets and aqueous urea solution droplets stabilized by hydrophobic silica particles, the DSC curves (*Fig. 12*) indicate a solidification signal I at T_c = –37°C very close to what was observed for the freezing of pure water droplets (*Fig. 12a*) and a solidification signal II at T_c = –52.6°C characteristic of the freezing of aqueous urea solution droplets with a concentration of 20wt% (*Fig. 12b*). DSC curves reveal that the evolution of the solidification signal occurs similarly to what is observed in the case of W/O mixed emulsions stabilized by a surfactant. Therefore these results evidence that aqueous urea solution droplets are diluted by the transfer of water from pure water droplets which progressively disappear from the mixed emulsion, in agreement with the previous studies presented. DSC cooling curves show no modification of the unique solidification peaks observed from 2 h characteristic of the complete water mass transfer. Similar experiments were performed on W/O mixed emulsions prepared in the same condition but containing pure water droplets and aqueous urea solution droplets stabilized by the non ionic Span80 surfactant. The same evolutions of the solidification signals are observed, but the unique solidification peak resulting for complete water mass transfer is observed after 1hour of evolution.

This work shows a water mass transfer through the oil media from the pure water droplets to the aqueous droplets containing a solute, causing their dilution. The transfer mechanism found is in agreement with the solution-diffusion model. This mechanism supposes that water can be solubilized in the oil medium and can also diffuse in this oil medium due to the composition discrepancy between the droplets that creates a chemical potential gradient. According to thermodynamic considerations, water transfer is expected from the pure water droplets (highest water chemical potential) toward the water + solute droplets (lowest water chemical potential),

and not the reverse. The results show that the characteristic time scale for water transport through the oil media can be about one hour in presence of surfactant. The kinetics of composition ripening seems to depend on parameters of emulsion formulation as the surfactant type and concentration, the solute type and concentration, and the presence of solid particles in the oil media. The mass transfer process is attributed to the great exchange area available in the emulsion and furthermore to the necessary presence of the surfactants. Although, the role of these parameters is not yet clearly established. These results evidence that the presence of silica particles in the oil media does not stop but slow down the water mass transfer, in comparison to a surfactant. These results suggest that the mechanism of mass transfer in presence of solid particles might be different of the solution-diffusion model previously proposed.

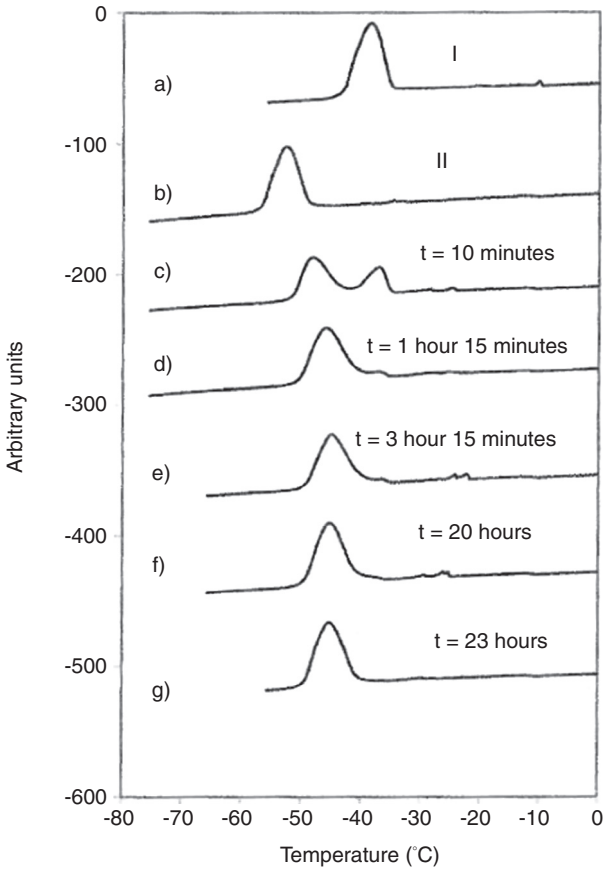

Figure 12

DSC cooling curves of W/O mixed emulsion with pure water droplets and (water + urea) droplets dispersed in oil media and stabilized by hydrophobic silica particles at successive time intervals a) corresponding W/O simple emulsion of water + urea droplets at $t = 0$; b) corresponding W/O simple emulsion of pure water droplets; c) $t = 10$ min; d) $t = 1$ h 15 min; e) $t = 3$ h 15 min; f) $t = 20$ h; g) $t = 23$ h (from [55]).

2.1.2 Mass Transfer Within Multiple Emulsions

W/O/W emulsions entrapping different compounds, urea or $MgSO_4$ have been studied by using the DSC technique. The release of tetradecane within an O/W/O multiple emulsion has also been studied by DSC and some of the results obtained are given thereafter. It is described how to detect the variations of composition of the external oil phases due to mass transfer, as a function of time.

The tetradecane/water/hexadecane (O1/W/O2) multiple emulsions were prepared in a two-step emulsification method [26]. Figure 13 is an example of the solidification curves obtained *versus* time. In this figure, the initial DSC curve was obtained by submitting the emulsion to cooling 1 minute after its preparation and it presents three peaks of crystallization. At that time, it is reasonable to consider that the transfer has not yet started and the three peaks of crystallization correspond to the crystallization of the three different phases composing the multiple emulsion. The signal at around –18°C represents the crystallization of the aqueous phase and it is characteristic of bulk water crystallization as it has been described previously. Even if the aqueous phase is dispersed as a multitude of globules, their size of around

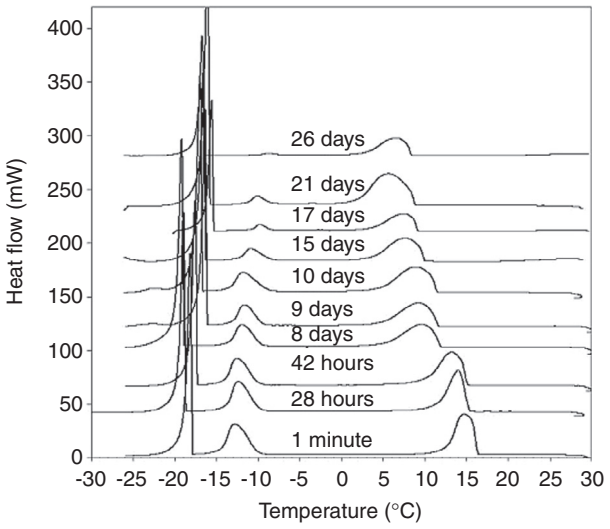

Figure 13

Evolution of the DSC curves of an O1/W/O2 tetradecane/water/hexadecane multiple emulsion containing 2 wt% of surfactant Tween 20 in the aqueous membrane.

1 mm is not sufficiently tiny to involve nucleation delays like those observed in W/O emulsions droplets of a few μm^3. Therefore the behavior of crystallization of aqueous globule looks like the crystallization of water bulk phase. The exothermic peak at 17°C in the initial part of the signal is sharp and is attributed to the bulk hexadecane crystallization. The hexadecane crystallizes at 17°C but with a very little degree of subcooling, its melting temperature being of 18°C. The third bell shape peak is attributed to the crystallization of the tetradecane dispersed droplets. The temperature is –12.8°C and is given by the apex of the peak which means that nearly 50% of the droplets are crystallized.

Figure 13 also shows a clear evolution with time of the crystallization peaks of the internal phase and the external phase. Actually, the crystallization peak of the tetradecane exhibits a progressive decrement in intensity whereas the temperature of the crystallization peaks of hexadecane decreases progressively from 17°C to 10°C. From these results it can be deduced that tetradecane releases gradually over time. On the ultimate DSC curve, the crystallization peak of tetradecane disappears which means that the globules are empty and all the tetradecane has been transferred in the external phase. Consequently the external phase composition has changed over time from pure hexadecane to a given tetradecane/hexadecane composition at the end of the transfer, passing through different intermediate compositions. From these experiments and the calibration curve that gives the solidification temperature of tetradecane *versus* temperature, it has been possible to determine the percentage of tetradecane still entrapped at time *t*. The values of the fraction of encapsulated tetradecane *versus* time obtained for different amounts of Tween20 (2, 4 and 7%) are reported in Figure 14.

The emulsions initially contained the same amount of encapsulated tetradecane and it can be easily observed that the kinetics depend on the amount of Tween 20 contained in the membrane. The higher the concentration of surfactant is, the faster the release of tetradecane is. Nevertheless, it must be emphasized that tetradecane is gradually released through the aqueous membrane and that no globule breaking was observed during the life time of the multiple emulsion.

A theoretical analysis has shown that the mass transfer occurs essentially by micellar diffusion [77].

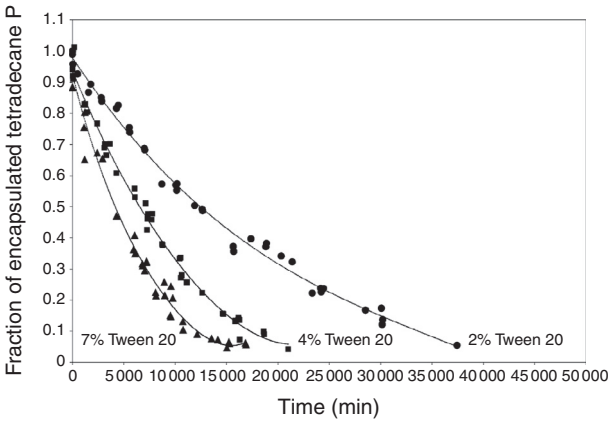

Figure 14

Evolution of the mass fraction of tetradecane encapsulated within the aqueous globule at different concentrations of Tween 20 in the aqueous membranes phase.

2.2 Crude Oil Emulsions in Production

Another application concerns the oil industry, and especially the liquid/liquid separation during crude oil exploitation.

In the oil industry, crude oil is always produced along with water. This produced water is mainly composed of formation water coming from the reservoir and from additional water that is often injected into the reservoirs to force the oil to the surface. As the field becomes depleted the produced water content of the oil tends to increase. During crude oil production, all conditions for the formation of stable emulsions are gathered, *i.e.* the presence of two non-miscible fluids (produced water and crude oil), zones of strong agitation to disperse one liquid into small droplets by turbulence or shear forces, and the presence of natural or added surfactants in the oil.

Very stable emulsions can be formed at the wellhead because of the sudden pressure drops that can occur in the choke valve or in the pumps. It is noteworthy that most of the crude oil emulsions formed in the field are of the W/O type. Nevertheless, O/W emulsions and multiple or complex emulsions (O/W/O or W/O/W) can also be encountered. In regular W/O oilfield emulsions, the dispersed aqueous phase is usually called "Sediment and Water" (S&W) and the continuous phase is crude oil. The dispersed S&W phase is essentially saline water, but may contain different types of solids. Crude oil emulsions vary from one field to another because crude oils differ by their geological age, chemical composition and associated impurities and furthermore, produced water exhibits physical and chemical properties which are also specific to each reservoir. Nevertheless, the common point for all the fields is that numerous surfactants or emulsifying agents are present in the produced fluids [78, 79]:

– indigenous surface active compounds such as asphaltenes and resins, that can play the role of high molecular weight surfactants;
– finely divided solids such as clay, sand, shale, silt, gilsonite, corrosion products, crystallized paraffins or waxes and precipitated asphaltenes and resins;
– chemical products used during production such as corrosion inhibitors, paraffin dispersants, biocides, cleaners and detergents, wetting agents, etc.

The emulsions formed can be very stable because of the presence of rigid films formed by polar compounds, such as asphaltenes and resins, and other fine solids which poses significant challenges during oil/water separation in surface production facilities [80-82]. Effective separation of crude oil and water is essential to ensure the quality of separated phases at the lowest cost. Crude-oil dehydration is generally accomplished by a combination of mechanical, electrical, thermal, and chemical methods. The addition of chemical additives is by far the most common method in emulsion breaking. The chemicals disrupt the interfacial film and enhance emulsion breaking.

Earlier studies [83, 84] have shown the importance of emulsion characteristics on the performance and optimization of oil/water separation. The main objective is to provide recommendations to reduce treatment costs and optimize oil/water separation in the field.

Crude oil emulsions are often difficult to characterize because of their opacity, their high water concentration (named "water cut" in oil production), the presence of various types of solids in both phases and the organic nature of the continuous phase. The determination of the droplet size distribution in oilfield emulsions is particularly important, because of the strong dependence between the rate of separation between crude oil and water and the size of the droplets. A knowledge of the drop size distribution is clearly an important factor in the design of separation equipment [81].

The study of the freezing behaviour of emulsions by microcalorimetry may provide useful qualitative information about their morphology. Firstly, it is particularly easy to differentiate a bulk phase from a dispersed one or to characterize the degree of polydispersity of an emulsion. Emulsion size may be modified during time, temperature cycles, crystallizations, mechanical stress or chemical reactivity for example. Qualitative information about alterations of emulsions may then be obtained by direct comparison of thermograms. So it is possible to study the influence of different agitation conditions on the drop size distributions of real samples of crude oil [62, 85-87] as shown in Figures 15 and 16. Figure 15 shows the DSC thermograms obtained from the analysis

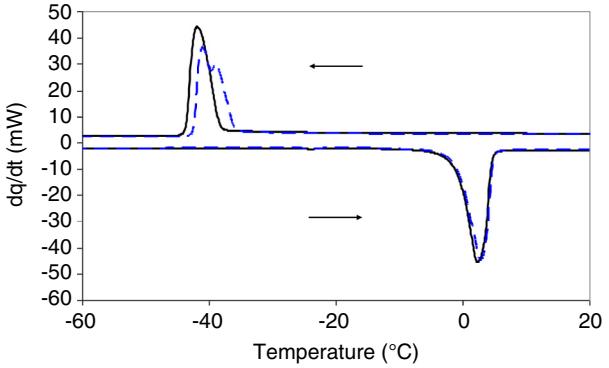

Figure 15

DSC thermograms of a heavy crude oil emulsion made with an *Ultra-Turrax* homogeniser (continuous line) or with a blade agitator (dotted line).

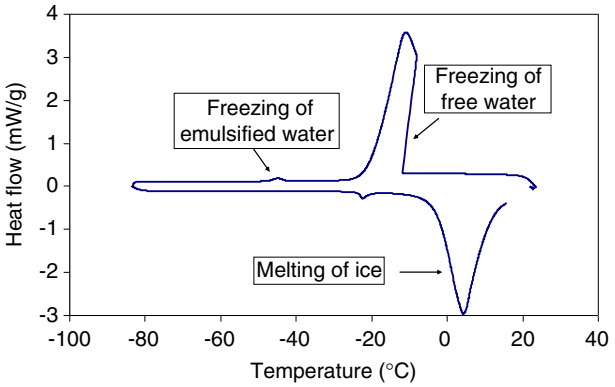

Figure 16

DSC thermogram of a multiple water-in-crude oil-in-water emulsion (from [87]).

of a heavy crude oil emulsion made with a high-shear device (*Ultra-Turrax* agitator) or with a low-shear blade agitator. The superimposition of both thermograms clearly underlines that the high-shear device causes the formation of water droplets that crystallize at lower temperatures, *i.e.* the average droplets size is smaller. Moreover, it is noteworthy that the thermogram of the blade-made emulsion shows two overlapping signals characteristic of a polydisperse emulsion. Figure 16 is an illustration of the occurrence of multiple emulsions when mixing crude oil and brine close to the inversion point, *i.e.* for a water phase fraction around 60%. The aqueous phase separated after the dispersion of crude oil and brine through a calibrated orifice used as a model choke valve was sampled and analysed by DSC.

The thermogram clearly shows a first exothermic signal around –15°C which is characteristic of the freezing of free water (continuous phase) but also a second very small exothermic signal around –40°C which underlines the freezing of emulsified water. This type of thermogram is characteristic of a multiple W/O/W emulsion, as it was confirmed by optical microscopy [87].

Microcalorimetry may be also very helpful to study the effect of a change of the aqueous phase composition on the morphology of emulsions, as it is the case in EOR (Enhanced Oil Recovery) applications, when chemicals are used to improve crude oil recovery. Chemical EOR operations consist in a combination of Surfactant and Polymer (SP) or Alkaline, Surfactant and Polymer (ASP) or variations of these two injection processes. As a matter of fact, EOR chemicals interact with reservoir fluids according to relatively complicated physical chemical mechanisms. Surfactants tend to decrease the oil/water InterFacial Tension (IFT), alkali saponifies indigenous acidic components in the crude, resulting in higher water solubility and lower IFT, and finally, polymers increase the viscosity of the aqueous phase. These phenomena may contribute to the formation of stable emulsions that may strongly differ from naturally occurring oilfield emulsions stabilized by indigenous polar components in the crude (resins, asphaltenes, etc.). A recent study presents an experimental investigation to underline the potential risk for emulsion formation in the framework of a chemical EOR operation (P, SP or ASP) and to quantify the impact of EOR chemicals on the efficiency of classical separation treatments (gravity separation, chemical demulsification and electrocoalescence) [88]. A diluted heavy oil system for which the interfacial behaviour has been previously studied in presence of alkali and surfactant was selected [89]. The stability of W/O emulsions formed in presence of alkaline (Na_2CO_3, pH11) and surfactant (Sodium Dodecyl Benzene Sulfonate, SDBS) under strong conditions of shearing was compared to emulsions formed with a brine at pH7. An analysis was performed with DSC to compare both types of emulsion (pH7 without surfactant and pH11). The thermograms in Figure 17 show that the signals of water melting obtained during heating are similar, which is expected because ice melts at constant temperature whatever the volume of the droplets in the emulsion. But it is noteworthy that during cooling, the exothermic signal of water freezing is very fine and centred around –40°C at pH11, while it is wider and shifted towards temperatures above –40°C at pH7. This analysis suggests that the emulsion formed at pH11 is monodisperse and contains very small water droplets, which was confirmed by cryo-SEM and Dynamic Light Scattering analysis.

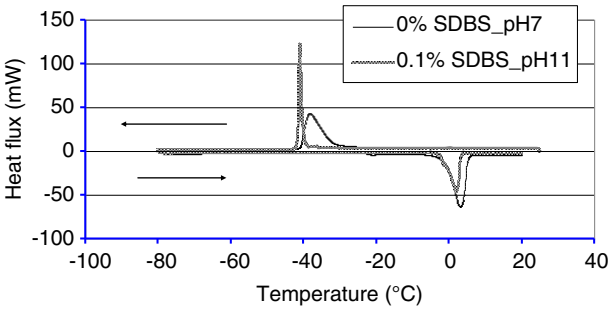

Figure 17

Thermograms of W/O emulsions. Black line: emulsion formed at pH7. Grey line: emulsion formed at pH11 with surfactant SDBS.

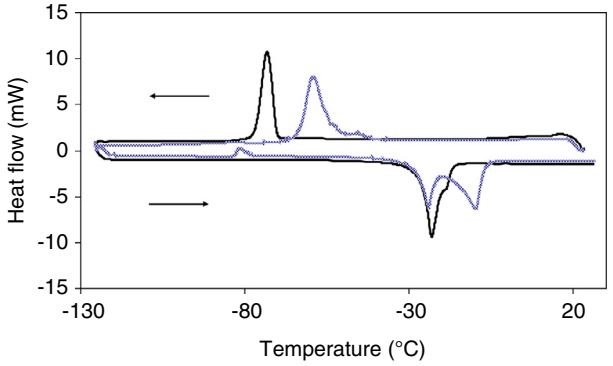

Figure 18

DSC thermograms of real oilfield emulsions. Black line: monodisperse W/O emulsion with a total salinity of 180 g/L. Grey line: polydisperse W/O emulsion with a total salinity of 110 g/L.

From a practical point of view, it is relatively easy to get a rapid signature of the morphology and composition of real emulsions directly sampled from the oilfield by using microcalorimetry [63, 90]. Figure 18 gives the example of 2 different W/O emulsions. The first thermogram (black line) shows a single regular peak of ice freezing during cooling at approximately –70°C, characteristic of a fine and monodisperse emulsion. The low value of the freezing temperature is due to the relatively high salinity of the aqueous phase, as shown by the melting signal. In fact, the melting peak is composed of two overlapping signals. The first one is the eutectic melting, around –20°C, which indicates that the main component of the brine is NaCl (the theoretical eutectic melting of the H_2O-NaCl sytem is at –21°C).

The second signal ends at around –18°C, which corresponds to a composition of 21% of NaCl in water for a pure binary system. These characteristics rapidly deduced from DSC analysis have been confirmed by cryo-SEM analysis which pointed out the occurrence of a monodisperse emulsion with an average diameter of 2 μm and by the results from the geochemical analysis of the associated water for which a total salinity of 180 g/L was found, the major salt being NaCl. The second thermogram (grey line) gives several exothermic peaks during cooling, indicating a polydisperse emulsion. The main peak at around –60°C is characteristic of finely emulsified water droplets but the other peaks that are observed as a shoulder of the main peak at higher temperature prove that large droplets are present in the emulsion. During melting, a first peak of eutectic melting is clearly observed around –20°C, immediately followed by the peak of progressive melting of ice which ends at –9°C, corresponding to a composition of 13% of NaCl in water for a purely binary system. Once again, the cryo-SEM analysis clearly confirmed the polydispersity of the emulsion (droplets size from 2 to 100 μm) and the geochemical analyses gave a total salinity of 110 g/L, very close to the approximate value deduced from DSC. In addition to these information, it is worth mentioning that it is possible to determine the approximate water content of the emulsion by integrating the melting signal in so far as samples of the associated free water phase are available in order to get a proper determination of the melting enthalpy. Of course, the quantity of emulsion analyzed by DSC being very small (a few mgs) it is recommended to confirm the water content by a Karl Fisher titration especially in the case of polydisperse systems [90].

Another interesting application of engineering concerns the field of emulsions breaking by electrocoalescence [87]. Electrostatic coalescers are generally used to efficiently separate small water droplets from crude oil, in the oilfield as in the refinery. The water molecule being polar, applying an electrical field to a water-in-oil emulsion permits to speed up the coalescence between droplets and to enhance the settling velocities in industrial gravity separators [78]. Recently, DSC was used to rapidly measure the efficiency of electrocoalescence in a specific prototype within the aim to evaluate the influence of several design parameter such as voltage, frequency, emulsion breaker concentration, residence time or temperature. The electrocoalescence efficiency E is defined from the evolution of the droplet size given by the DSC analysis of the emulsion before and after applying the electrical stress. As shown on the typical thermograms presented in Figure 19a and 19b, A_0 is the freezing energy of the tiny–droplets peak of the initial emulsion and A_f is the freezing energy of the tiny-droplets peak still present in the emulsion after applying the electrical stress. This energy is calculated from the integration of the peak area. The efficiency of electrocoalescence is given by the following equation:

$$E = 1 - (A_f/A_0) \tag{10}$$

Finally, it is noteworthy that quantitative information on the granulometry of emulsions may also be deduced from data obtained during crystallization and in fact

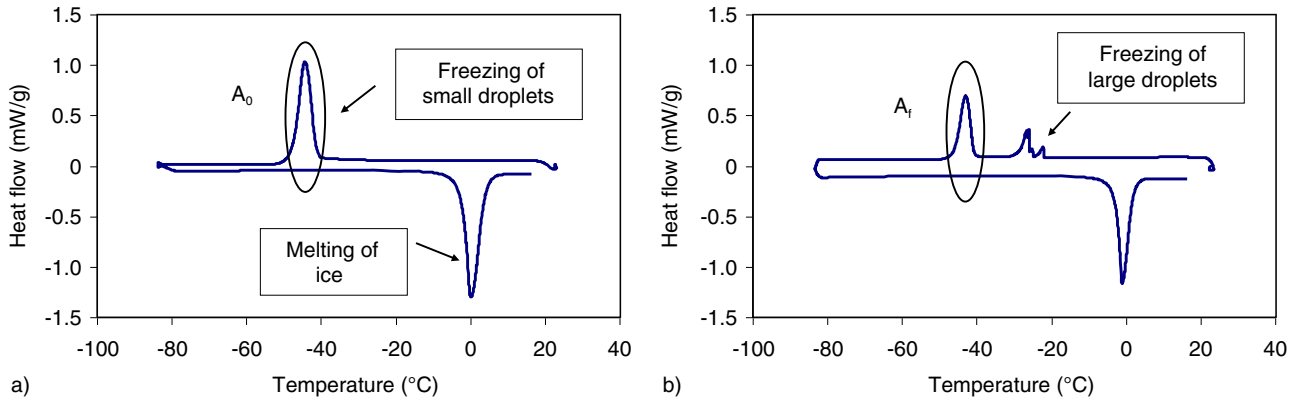

Figure 19

Typical DSC thermograms of the W/O emulsion a) before and b) after the application of the electrical field in the coalescer device (from [87]).

nucleation inside droplets. Two possibilities exist. First, one may derive an equation between the crystallization temperature of a droplet and its size from theoretical consideration, as it has been described by [62, 86]. This theoretical approach is based on the fact that to induce freezing, the formation of an ice germ is required. Due to capillary phenomena, it is possible to demonstrate that the relation between the water droplet radius r and the freezing temperature T^* is given by the following equation:

$$r^3 = -\frac{3\dot{T}}{4\pi}\frac{0.69}{\int_{T_m}^{T^*} J dT} \tag{11}$$

with the nucleation rate J given by:

$$J = A \exp\left[\frac{16\pi\gamma^3 V_i^2}{3L_m^2 \ln^2\left(\frac{T}{T_m}\right)}\frac{1}{kT}\right] \tag{12}$$

where $\dot{T}$ (K.s^{-1}) is the scanning rate, A (s^{-1}.m^{-3}) is the pre exponential factor in the expression of the nucleation rate, k (N.m.K^{-1}) is the Boltzmann constant, γ (N.m^{-1}) is the interfacial tension between water and the ice germ, V_i (m^3.mole^{-1}) is the molar volume of the germ, L_m (N.m.mole^{-1}) is the molar melting heat and T_m (K) is the melting temperature.

So it is clear from Equation (11) that the relation between r and T^* is far from direct, and the difficulty is essentially due to the impossibility to determine γ from an experimental point of view. That is the reason why it is preferable to determine an empirical correlation between r and T^* by comparing the most probable freezing temperatures obtained from DSC thermal analysis and the mean droplet size obtained by another analytical technique (optical microscopy for instance). Applications of thermogranulometry for crude oil emulsions may be found in [86, 91].

CONCLUSION

Freezing behavior of emulsions can be easily exploited to characterize dispersed systems which can be very complex, such as simple, multiple or mixed emulsions. In this article, we recall the theoretical aspects of nucleation that permit to establish a correlation between the solidification temperature of the emulsion droplets and their size, in the case of pure compounds as in the case of more complex materials like aqueous solutions. The DSC technique is particularly useful and relevant for studying the evolution of such emulsions. Application examples in the field of mass transfer or liquid/liquid separation are presented and detailed in order to show the many possibilities offered by microcalorimetry to characterize complex systems that have an interest in the field of industry and engineering.

ACKNOWLEDGMENTS

The authors wish to thank *ESA* for financial support of MAP-project FASES and for support of PASTA project (continuation of FASES).

REFERENCES

1 Becher P. (1982) *Encyclopedia of Emulsion Technology*, Marcel Dekker, New York.

2 Lissant K.J. (1974) *Emulsions and Emulsion Technology,* Surfactant Science Series, Vol. **6**, Marcel Dekker, New York.

3 McClements D.J. (1999) *Food emulsions: Principles, Practice, and Techniques*, CRC Series in contemporary food science, CRC Press, Boca Raton.

4 Sjöblom J. (1992) *Emulsion – A Fundamental and Practical Approach*, NATO ASI Series, Kluwer Academic Publishers, Dordrecht.

5 Tadros T.F. (2007) *Colloid stability and application in pharmacy*, Colloids and Interface Science Series, Vol. **3**, Tadros T.F. (ed.), Wiley-VCH, Weinheim.

6 Clausse D. (1985) Research techniques utilizing emulsions, in *Encyclopaedia of Emulsion Technology*, Vol. **2**, pp. 77-157, Becher P. (ed.), Marcel Dekker, New York.

7 Grossiord J.L., Seiller M., Silva-Cunha A. (1998) Obtaining multiple emulsions, in *Multiple emulsions: structure, properties and applications*, Seiller M., Grossiord J.L. (eds), Édition de santé, Paris, France, pp. 57-80, ISBN 2-86411-119-5.

8 Grossiord J.L., Stambouli M. (2007) Potentialities of W/O/W Multiple Emulsions in Drug Delivery and Detoxification, in *Multiple Emulsion: Technology and Applications*, Aserin A. (ed.), John Wiley and Sons Inc., Hoboken, USA, pp. 209-234, ISBN 978-0-470-17093-9.

9 Garti N., Lutz R. (2004) Recent progress in double emulsion, in *Emulsions: Structure Stability and Interactions,* Petsev D.N. (ed.), Elsevier, Oxford, UK, pp. 557-667, ISBN 0-12-088499-2.

10 Noble R.D., Stern A.A. (1995) *Membrane separation technology: Principle and application*, Elsevier Science, Amsterdam, The Netherlands, ISBN 044481633X.

11 Benichou A., Aserin A. (2007) Recent developments in O/W/O multiple emulsions, in *Multiple Emulsion: Technology and Applications,* Aserin A. (ed.), John Wiley and Sons Inc, Hoboken, USA, pp. 165-208, ISBN 978-0-470-17093-9.

12 Li N.N. (1968) Membrane Separation Process, *US Patent* 3 410 794.

13 Garti N., Kovacs A. (1991) Facilitated emulsion liquid membrane separation of complex hydrocarbon mixtures, *J. Membr. Sci.* **56**, 3, 239-246, ISSN 0376-7388.

14 Kaghazchi T., Kargari A., Yegani R., Zare A. (2006) Emulsion liquid membrane pertraction of L-lysine from dilute aqueous solutions by D2EHPA mobile carrier, *Desalination* **190**, 1-3, 161-171, ISSN 0011-9164.

15 Krishna R., Goswami A.N., Sharma A. (1987) Effect of emulsion breakage on selectivity in the separation of hydrocarbon mixtures using aqueous surfactant membranes, *J. Membr. Sci.* **34**, 2, 141-154, ISSN 0376-7388.

16 Kumbasar R.A. (2009) Extraction and concentration study of cadmium from zinc plant leach solutions by emulsion liquid membrane using trioctylamine as extractant, *Hydrometallurgy* **95**, 3-4, 290-296, ISSN 0304-386X.

17 Laugel C., Baillet A., Youenang Piemi M.P., Marty J.P., Ferrier D. (1998) Oil–water–oil multiple emulsion for prolonged delivery of hydrocortisone after topical application: comparison with simple emulsion, *Int. J. Pharm.* **160**, 1, 109-117, ISSN 0378-5173.

18 Laugel C., Rafidison P., Potard G., Aguadisch L., Baillet A. (2000) Modulated release of triterpenic compounds from a O/W/O multiple emulsion formulated with dimethicones: infrared spectrophotometric and differential calorimetric approaches, *J. Control. Release* **63**, 1-2, 7-17, ISSN 0168-3659.

19 Mishra B., Pandit J.R. (1989) Prolonged release of pentazocine from multiple O/W/O emulsions, *Drug Dev. Ind. Pharm.* **15**, 8, 1217-1230, ISSN: 0363-9045.

20 Mortaheb H.R., Aminia M.H., Sadeghiana F., Mokhtarania B., Daneshyara H. (2008) Study on a new surfactant for removal of phenol from wastewater by emulsion liquid membrane, *J. Hazardous Mater.* **160**, 2-3, 582-588, ISSN 0304-3894.

21 Ng Y.S., Jayakumar N.S., Hashim M.A. (2010) Performance evaluation of organic emulsion liquid membrane on phenol removal, *J. Hazardous Mater.* **184**, 1-3, 255-260, ISSN 0304-3894.

22 Tedajo G.M., Seiller M., Prognon P., Grossiord J.L. (2001) pH compartmented W/O/W multiple emulsion: a diffusion study, *J. Control. Release* **75**, 1-2, 45-53, ISSN 0168-3659.

23 Tedajo G.M., Bouttier S., Fourniat J., Grossiord J.-L., Marty J.P., Seiller M. (2005) Release of antiseptics from the aqueous compartments of a W/O/W multiple emulsion, *Int. J. Pharm.* **288**, 1, 63-72, ISSN 0378-5173.

24 Hasan M.A., Selim Y.T., Mohamed K.M. (2006) Removal of chromium from aqueous waste solution using liquid emulsion membrane, *J. Hazardous Mater.* **168**, 2-3, 1537-1541, ISSN 0304-3894.

25 Hai M., Magdassi S. (2004) Investigation on the release of fluorescent markers from W/O/W emulsions by fluorescence-activated cell sorter, *J. Control. Release* **96**, 3, 393-402, ISSN 0168-3659.

26 Avendaño-Gomez J.R., Grossiord J.L., Clausse D. (2005) Study of mass transfer in oil–water–oil multiple emulsion by differential scanning calorimetry, *J. Colloid Interface Sci.* **290**, 2, 533-545, ISSN 0021-9797.

27 Clausse D., Pezron I., Raynal S. (1995) Water transfer within multiple W/O/W emulsions at a fixed subambiant temperature, *Cryo-Letters* **16**, 4, 219-230, ISSN 0143-2044.

28 Clausse D., Pezron I., Komunjer L. (1999) Stability of W/O and W/O/W emulsions as a result of partial solidification, *Colloids Surf. A: Physicochem. Eng. Aspects* **152**, 1-2, 23-29, ISSN 0927-7757.

29 Frasca S., Couvreur P., Seiller M., Pareau D., Lacour B., Stambouli M., Grossiord J.L. (2009) Paraquat detoxication with multiple emulsions, *Int. J. Pharm.* **380**, 1-2, 142-146, ISSN 0378-5173.

30 Geiger S., Tokgoz S., Fructus A., Jager-Lezer N., Seiller M., Lacombe C., Grossiord J.L. (1998) Kinetics of swelling–breakdown of a W/O/W multiple emulsion: possible mechanisms for the lipophilic surfactant effect, *J. Control. Release* **52**, 1-2, 99-107, ISSN 0168-3659.

31 Lutz R., Aserin A., Wicker L., Garti N. (2009) Release of electrolytes from W/O/W double emulsions stabilized by a soluble complex of modified pectin and whey protein isolate, *Colloids Surf. B: Biointerfaces* **74**, 1, 178-185, ISSN 0927-7765.

32 Muschiolik G. (2007) Multiple emulsions for food use, *Curr. Opin. Colloid Interface Sci.* **12**, 4-5, 213-220, ISSN 1359-0294.

33 Muguet V., Seiller M., Barratt G., Ozer O., Marty J.P., Grossiord J.L. (2001) Formulation of shear rate sensitive multiple emulsions, *J. Control. Release* **70**, 1-2, 37-49, ISSN 0168-3659.

34 Venkatesan S., Sheriffa Meera, Begum K.M. (2009) Emulsion liquid membrane pertraction of benzimidazole using a room temperature ionic liquid (RTIL) carrier, *Chem. Eng. J.* **148**, 2-3, 254-262, ISSN 1385-8947.

35 Yan J., Pal R. (2001) Osmotic swelling behavior of globules of W/O/W emulsion liquid membranes, *J. Membr. Sci.* **190**, 1, 79-91, ISSN 0376-7388.

36 Yan J., Pal R. (2004) Effects of aqueous-phase acidity and salinity on isotonic swelling of W/O/W emulsion liquid membranes under agitation conditions, *J. Membr. Sci* **244**, 1-2, 193-203, ISSN 0376-7388.

37 Yu S.C., Bochot A., Le Bas G., Chéron M., Mahuteau J., Grossiord J.L., Seiller M., Duchêne D. (2009) Effect of camphor/cyclodextrin complexation on the stability of O/W/O multiple emulsion, *Int. J. Pharm.* **261**, 1-2, 1-8, ISSN 0378-5173.

38 Colinart P., Delepine S., Trouve G., Renon H. (1984) Water transfer in emulsified liquid membrane process, *J. Membr. Sci.* **20**, 2, 167-187, ISSN 0376-7388.

39 Potier L., Raynal S., Seiller M., Grossiord J.L., Clausse D. (1992) Study state transitions within multiple W/O/W emulsions using calorimetry (DSC), *Thermochim. Acta* **204**, 1, 145-155, ISSN 25 0040-6031.

40 Potier L. (1993) Étude par calorimétrie des changements d'état dans une émulsion multiple E/H/E : application aux transferts de solvant entre deux phases aqueuses, *Thèse*, Université de Technologie de Compiègne, France.

41 Drelich A. (2009) Émulsions formulées avec des particules de silice : caractérisation, stabilité, transfert de matière, *Thèse*, Université de Technologie de Compiègne, France.

42 Drelich A., Gomez F., Clausse D., Pezron I. (2010) Evolution of water-in-oil emulsions stabilized with solid particles Influence of added emulsifier, *Colloids Surf. A: Physicochem. Eng. Aspects* **365**, 1-3, 171-177.

43 Avendaño-Gomez J., Grossiord J.L., Clausse D. (2000) Composition ripening in o/w emulsions, *Entropie* **36**, 224-25, 110-116, ISSN 0013-9084.

44 Avendaño-Gomez J. (2002) Étude par calorimétrie du mûrissement de composition dans une émulsion mixte H1-H2/eau et une émulsion multiple H1/eau/H2, *Thèse*, Université de Technologie de Compiègne, France.

45 Chebab M.B., Benna M., Trabelsi-Ayadi M., Clausse D. (2011) Study by Differential Scanning Calorimetry of Water-in-Oil Emulsions Stabilized by Clays and CTAB, *J. Dispers. Sci. Technol.* **32**, 1-3, 67-76.

46 Binks B.P., Clint J.H., Fletcher P.D.I., Rippon S. (1998) Kinetics of swelling of oil-in-water emulsions, *Langmuir* **14**, 19, 5402-5411, ISSN 0743-7463.

47 Binks B.P., Clint J.H., Fletcher P.D.I., Rippon S., Lubetkin S.D., Mulqueen P.J. (1999) Kinetics of swelling of oil-in-water emulsions stabilized by different surfactants, *Langmuir* **15**, 13, 4495-4501, ISSN 0743-7463.

48 Clausse D., Pezron I., Gauthier A. (1995) Water transfer in mixed water-in-oil emulsions studied by differential scanning calorimetry, *Fluid Phase Equilibr.* **110**, 1-2, 137-150, ISSN 0378-3812.

49 Clausse D., Pezron I., Behaeghel A. (1999) Water transfer between water and water + NaCl droplets in emulsions, *J. Dispers. Sci. Technol* **20**, 1-2, 315-326, ISSN 0193-2691.

50 Clausse D., Fouconnier B., Avendaño-Gomez J.R. (2002) Ripening phenomena in Emulsions - A calorimetry investigation, *J. Dispers. Sci. Technol.* **23**, 1-3, 379-391, ISSN 0193-2691.

51 Clausse D., Drelich A., Fouconnier B. (2011) Mass Transfers Within Emulsions Studied by Differential Scanning Calorimetry (DSC) - Application to Composition Ripening and Solid Ripening, Mass Transfer - Advanced Aspects, Dr. Hironori Nakajima (ed.), ISBN: 978-953-307-636-2, InTech, DOI: 10.5772/20279. Available from: http://www.intechopen.com/books/mass-transfer-advanced-aspects/mass-transfers-within-emulsions-studied-by-differential-scanning-calorimetry-dsc-application-to-comp

52 Elwell M.W., Roberts R.F., Coupland J.N. (2004) Effect of homogenization and surfactant type on the exchange of oil between emulsion droplets, *Food Hydrocol.* **18**, 3, 413-418, ISSN 0268-005X.

53 McClements D.J., Dungan S.R., German J.B., Kinsella J.E. (1993) Factors which affect oil exchange between oil-in-water emulsion droplets stabilized by whey protein isolate: protein concentration, droplet size and ethanol, *Colloids Surf. A: Physicochem. Eng. Aspects* **81**, 13, 203-210, ISSN 0927-7757.

54 McClements D.J., Dungan S.R. (1993) Factors that affect the rate of oil exchange between oil-in-water emulsion droplets stabilized by a non-ionic surfactant: droplet size, surfactant concentration, and ionic strength, *J. Phys. Chem.* **97**, 28, 7304-7308, ISSN 0022-3654.

55 Sacca L., Drelich A., Gomez F., Pezron I., Clausse D. (2008) Composition Ripening in Mixed Water-in-oil Emulsions Stabilized with Solids Particles, *J. Dispers. Sci. Technol.* **29**, 7, 948-952, ISSN 0193-2691.

56 Taisne L., Walstra P., Cabane B. (1996) Transfer of oil between emulsion droplets, *J. Colloid Interface Sci.* **184**, 2, 378-390, ISSN 0021-9797.

57 Weiss J., Cancelliere C., McClements D.J. (2000) Mass Transport Phenomena in Oil-in-Water Emulsions Containing Surfactant Micelles: Ostwald Ripening, *Langmuir* **16**, 17, 6833-6838, ISSN 0743-746.

58 Passerone A., Liggieri L., Miller R., Clausse D., Steinchen A., Loglio G., Di Lullo A. (2002) The FASES project for the investigation of emulsion stability in microgravity, *Third world congress on emulsions*, Lyon, France, 24-27 Sept.

59 Clausse D., Pezron I., Gomez F., Dalmazzone C., Sacca L., Drelich A. (2008) Differential Scanning Calorimetry as a tool for following emulsion evolution in microgravity conditions from the MAP-Project FASES, *J. Jpn Soc. Microgravity Application* **25**, 3, 227-230.

60 Broto F., Clausse D. (1976) A study of the freezing of supercooled water dispersed within emulsions by DSC, *J. Phys. C: Solid State Phys.* **9**, 4251-4257.

61 Clausse D. (1985) Caractérisation des propriétés thermodynamiques d'une émulsion. Détermination de la température et de l'enthalpie de changement d'état de la phase dispersée, *Revue Générale de Thermique* **279**, 263-268, ISSN 0035-3159.

62 Clausse D., Gomez F., Pezron I., Komunjer L., Dalmazzone C. (2005) Morphology characterization of emulsions by differential scanning calorimetry, *Adv. Colloid Interface Sci.* **117**, 1-3, 59-74, ISSN 0001-8686.

63 Dalmazzone C., Noïk C., Clausse D. (2009) Application of DSC for emulsified system characterization, *Oil Gas Sci. Technol.* **64**, 5, 543-555.

64 Franks F. (1982) *Water: a comprehensive treatise, Vol. 7: water and aqueous solutions at subzero temperatures*, Franks F. (ed.), Plenum Press, New York and London.

65 Clausse D. (1998) Thermal behaviour of emulsions studied by Differential Scanning Calorimetry, *J. Thermal Anal.* **51**, 191-201.

66 Dufour L., Defay R. (1963) Thermodynamics of clouds, in *International Geophysics Series Vol. 6*, Van Mieghem J. (ed.), Academic Press, New York and London.

67 Mutaftschiev B. (2001) *The atomic nature of crystal growth*, Materials Science Series, Springer-Verlag, Berlin, Heidelberg, New York, ISBN 3-540-66496-3.

68 Pruppacher H., Klett J.D. (1978) *Microphysics of clouds and precipitation*, Kluwer Academic Publishers, Dordrecht, The Netherlands.

69 Kashchiev D., Clausse D., Jolivet-Dalmazzone C. (1994) Crystallization and critical supercooling of disperse liquids, *J. Colloid Interface Sci.* **165**, 1, 148-153.

70 Kashchiev D. (2000) *Nucleation-Basic theory with applications*, Butterworth-Heinemann, Oxford, ISBN 0750646829.

71 Zettlemoyer A.C. (1969) *Nucleation*, Zettlemoyer A.C. (ed.), Marcel Dekker, New York.

72 Turnbull D. (1952) Kinetics of solidification of supercooled liquid mercury droplets, *J. Chem. Phys.* **20**, 411-424.

73 Wagner P.E. (1988) Atmospheric Aerosols and Nucleation, *Twelfth International Conference on Atmospheric Aerosols and Nucleation*, University of Vienna, Austria, 22-27 Aug., Vali G. (ed.), Lectures notes in Physics 309, Springer-Verlag, Berlin and Heidelberg.

74 Broto F., Clausse D., Babin L., Mercier M. (1978) Détermination par microscopie électronique de la granulométrie d'une émulsion d'eau et corrélation entre la cristallisation des gouttes et leurs diamètres, *Journal de Chimie et Physique* **75**, 908-910.

75 Clausse D., Babin L., Broto F., Aguerd M., Clausse M. (1983) Kinetics of ice nucleation in aqueous solutions, *J. Phys. Chem.* **87**, 4030-4034.

76 Clausse D., Dumas J.P., Meijer P.H.E., Broto F. (1987) Phase transformations in emulsions. Part 1: Effects of thermal treatments on nucleation phenomena. Experiments and models, *J. Dispers. Sci. Technol.* **8**, 1-28.

77 Stambouli M., Avendano-Gomez J.R., Pezron I., Pareau D., Clausse D., Grossiord J.L. (2007) Modelization of the release from a tetradecane/water/hexadecane multiple emulsion: Evidence of significant micellar diffusion, *Langmuir* **23**, 3, 1052-1056, ISSN 0743-7463.

78 Manning F.S., Thompson R.E. (1995) *Oilfield Processing Volume 2: Crude Oil*, Pennwell Publishing Company, Tulsa, pp. 39-60.

79 Svetgoff J.A. (1988) Demulsification Key to Production Efficiency, *Petrol. Eng. Int.* **61**, 28-37.

80 Kokal S.L. (2006) Crude Oil Emulsions, in *Petroleum Engineering Handbook, Vol. 1—General Engineering*, Fanchi J.R. (ed.), Society of Petroleum Engineers, Richardson, Texas.

81 Kokal S.L. (2005) Crude Oil Emulsions: A State of the Art Review, *SPE Prod. Facil.* **20**, 1, 5-13.

82 Schramm L.L. (1992) Petroleum Emulsions – Basic principles, in *Emulsions-Fundamentals and Applications in the Petroleum Industry*, Schramm L.L. (ed.), Advances in Chemistry Series 231, American Chemical Society, Washington, DC.

83 Kokal S., Al-Ghamdi A. (2007) An Investigative Study of Potential Emulsion Problems Before Field Development, *SPE Proj. Fac. Const.* **2**, 1, 1-10. SPE-102856-PA.

84 Kokal S., Al-Ghamdi A. (2008) Performance Appraisals of Gas Oil Separation Plants, *SPE Prod. Oper.* **23**, 2, 287-296. SPE-102854-PA.

85 Dalmazzone C., Clausse D. (2001) Microcalorimetry, in *Encyclopedic Handbook of Emulsion Technology*, Ch. 14, Sjöblom J. (ed.), Marcel Dekker, New York.

86 Clausse D., Gomez F., Dalmazzone C., Noik C. (2005) A method for the characterization of emulsions: Thermogranulometry. Application to water-in-crude oil emulsion, *J. Colloid Interface Sci.* **287**, 694-703.

87 Dalmazzone C., Noïk C., Glénat P., Dang F. (2010) Development of a methodology for the optimization of dehydration of extraheavy oil emulsions, *SPE J.* **15**, 3, 726-736.

88 Dalmazzone C., Noïk C., Argillier J.F. (2012) Impact of Chemical EOR on the Separation of Diluted Heavy oil Emulsions, *Energy Fuels* **26**, 3462-3469.

89 Trabelsi S., Argillier J.-F., Dalmazzone C., Hutin A., Bazin B., Langevin D. (2011) Effect of Added Surfactants in an Enhanced Alkaline/heavy oil System, *Energy Fuels* **25**, 1681-1685.

90 Al-Ghamdi A.M., Noik C., Dalmazzone C., Kokal S. (2009) Experimental Investigation of Emulsion Stability in Gas/Oil Separation Plants, *SPE J.* **14**, 4, 595-605.

91 Diaz-Ponce J.A., Flores E.A., Lopez-Ortega A., Hernandez-Cortez J.G., Estrada A., Castro L.V., Vazquez F. (2010) Differential scanning calorimetry characterization of water-in-oil emulsions from Mexican crude oils, *J. Therm. Anal. Calorim.* **102**, 899-906.

Manuscript accepted in April 2013
Published online in November 2013